

Reprinted from

JOURNAL OF HYDROLOGY

Journal of Hydrology 217 (1999) 285–302

Scale dependencies of hydrologic models to spatial variability of precipitation

V.I. Koren*, B.D. Finnerty, J.C. Schaake, M.B. Smith, D.-J. Seo, Q.-Y. Duan

Office of Hydrology, National Weather Service, NOAA, 1325 East-West Highway, Silver Spring, MD 20910, USA

Received 22 December 1997; accepted 10 September 1998



ELSEVIER

(WCRP, 1992; Entekhabi and Eagleson, 1989) when surface–atmosphere interactions occur at different scales (Avisar, 1995). Modeling of the feedback processes in the water and energy exchanges between the land surface and atmosphere requires an understanding of the scale-dependent behavior of the rainfall-runoff model. An accurate representation of the hydrologic cycle across a range of scales is also important to general weather and climate forecasts and for water resources planning and management.

Field observations have shown that the major sources of heterogeneity leading to spatial differences in runoff are topography, soils, and rainfall (Wood et al., 1990). Basin topography and soils are practically time invariant, but spatial rainfall patterns vary in time introducing more complexity into rainfall-runoff modeling. Hydrologic models have been widely used to investigate the natural scale-dependent behavior of the rainfall-runoff process. Numerical experiments have shown modeled runoff to be highly scale dependent. However, the model results varied widely according to the rainfall-runoff model being utilized.

Runoff scaling experiments by Finnerty et al. (1997) clearly showed the sensitivity of Sacramento model runoff generation to spatial and temporal averaging of rainfall inputs using 7 months of NEXRAD radar data. The Sacramento model has both a threshold triggering mechanism for runoff that is a function of soil moisture storage as well as an infiltration component which is a function of rainfall intensity and soil moisture content. Numerous other experiments have shown that simulated runoff is sensitive to the space–time scales of precipitation inputs (Loague, 1988; Kouwen and Garland, 1989; Beven and Wood, 1993; Ogden and Julien, 1994; Shah, 1996). Most of these models are formulated with a rainfall rate sensitive infiltration-excess mechanism to partition rainfall into runoff. However, conflicting results by Obled et al. (1974), using saturation-excess type runoff models such as TOPMODEL, have shown that runoff is not very sensitive to spatial scale. These conflicting results can be largely explained by the runoff mechanism in the individual model formulations, and the space–time scales used in the experiments.

This paper addresses a wide range of scales which are representative of the scales generally used for operational flood forecasting, climate modeling, and

common lumped parameter basin modeling. The paper continues the work by Finnerty et al. (1997) by addressing the sensitivity of the runoff models themselves to rainfall averaging. A possible solution to the runoff scale problem is presented in a reformulated version of the Sacramento model which was developed to reduce the scale dependency of the runoff, without sacrificing complexity in the hydrologic formulation. Extension of the input radar data set to over three years provides for long-term continuous simulations and robust statistics that are representative of general model behavior. Herein is presented a means to identify natural scale dependency of the runoff processes from the scale dependent behavior of the runoff model, and relate the results directly to the specific runoff generating mechanisms employed by a variety of commonly used hydrologic models.

2. Model scale

Historically, less emphasis has been placed on the scale dependency inherent in the rainfall-runoff model as opposed to the scale of rainfall. Analysis of the spatial variability of rainfall can give a qualitative sense of this scale dependency, however, quantitative measures of physical scale are highly model dependent. For example, the linear rainfall-runoff relationship in Eq. (1) is not sensitive to the spatial variability of rainfall given that the spatial averages of rainfall preserve the total volume of precipitation:

$$\bar{R}_A^{(k)} = a(t)\bar{P}_A \quad (1)$$

where $\bar{R}_A^{(k)}$ is runoff averaged over an area A using scale k estimates of runoff, \bar{P}_A is a mean areal rainfall, and $a(t)$ is the scale-independent parameter for the rainfall-runoff relationship.

The rainfall-runoff model, however, becomes scale dependent if, for example, its parameter is a linear function of the rainfall rate P_i :

$$R_i = b(t)P_i P_i = b(t)P_i^2 \quad (2)$$

Runoff from an area A (say, a river basin) can be aggregated from runoffs simulated at a finer scale, R_i ,

$$\bar{R}_A^{(k)} = \frac{1}{N_k} \sum_{i=1}^{N_k} R_i^{(k)} \quad (3)$$

Table 1

Averaged hourly values of rainy area fraction and coefficient of rainfall variation at different grid scales

Scale, km	4 × 4	8 × 8	16 × 16	32 × 32	64 × 64	128 × 128	256 × 256
Coefficient of variation	2.07	1.99	1.85	1.63	1.30	0.85	
Covered area, %	100	98	95	89	79	64	45

where N_k is a number of k -scale elements in the area A . Combination of Eqs. (2) and (3) leads to

$$\bar{R}_A^{(k)} = b^{(k)}(t) \frac{1}{N_k} \sum_{i=1}^{N_k} (P_i^{(k)})^2 = b^{(k)}(t) \left[(\sigma^{(k)})^2 + (\bar{P}^{(k)})^2 \right] \quad (4)$$

where $\sigma^{(k)}$ is the spatial standard deviation of rainfall averaged over scale k , and $\bar{P}^{(k)}$ is the mean value of k -scale rainfall that is equal to the rainfall averaged over an entire area, \bar{P}_A . For a scale-independent unbiased model the right-hand side of Eq. (4) should be the same at any scale less than the area A . This leads to a relationship between the model parameter $b^{(k)}(t)$ at different scales. Substituting a coefficient of rainfall variation, $C_v^{(k)}$, instead of a standard deviation, gives

$$b^{(k+n)}(t) = b^{(k)}(t) \frac{1 + (C_v^{(k)})^2}{1 + (C_v^{(k+n)})^2} \quad (5)$$

Eq. (5) shows how to preserve a constant average runoff over an area A by adjusting the model parameter $b^{(k)}(t)$. The adjustment depends on differences

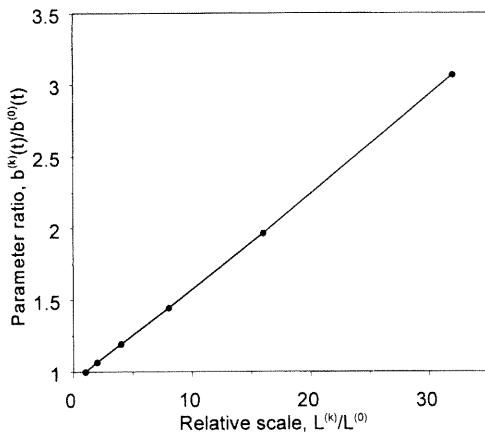


Fig. 1. Scale dependency of a point type rainfall runoff model parameter, $b^{(k)}(t)$, which is constant for a given scale, k and varies across scales as a function of rainfall variability.

of rainfall variability at different scales. The coefficient of spatial variation of precipitation can vary significantly at different averaging scales. Table 1 is an example of the scale dependency of the coefficient of variation and the rainy area fraction. The statistics were derived from Stage III data over a 256×256 km region in the southern plains of the United States for the 3-year period. Rainy area fractions and coefficients of variation were estimated at each hourly time interval and were weighted by the region average rainfall at that interval, while averaging for the 3-year period.

The model parameter $b^{(k)}(t)$ will vary greatly from scale to scale following significant differences of the coefficient of variation. Fig. 1 plots the ratio of $b^{(k)}(t)/b^{(0)}(t)$ versus $L^{(k)}/L^{(0)}$, where $L^{(0)}$ is the finest resolution of the radar estimates ($4 \text{ km} \times 4 \text{ km}$), $L^{(k)}$ is the k -scale, $b^{(0)}$ is the coefficient at the finest resolution, and $b^{(k)}$ is the coefficient at the k -scale. The parameter $b^{(k)}(t)$ in this plot was derived from Eq. (5) using the data in Table 1. Fig. 1 clearly illustrates that the coefficient in Eq. (2) changes significantly from scale to scale.

A sensitivity analyses of the Sacramento soil moisture accounting (SAC-SMA) model Burnash (1995) to the space–time variability of rainfall was presented in Finnerty et al. (1997). The high resolution NEXRAD Stage III precipitation estimates were used in the analyses. That study showed that well calibrated and unbiased SAC-SMA model parameters will produce biased runoff if the model is applied at scales different from that on which the model was calibrated. The results of Finnerty et al. (1997) indicate the scale issues illustrated in Fig. 1 and suggest a need for the approach shown in Eq. (5).

3. Hydrologic models analyzed

This study is focused on comparative analyses of scale dependency of lumped hydrological models

with different formulations of the infiltration processes. Three lumped hydrological models of differing complexity were used in the study: the SAC-SMA model, the Oregon State University (OSU) multi layer model (Mahrt and Pan, 1984), and the simple water balance (SWB) model (Schaake et al., 1996). The first two models are typical point models that do not account for the spatial variability within the basin. The SWB model implicitly accounts for the spatial variability in precipitation data and model states. A fourth model, a reformulated version of the SAC-SMA model which accounts for the spatial variability of rainfall only, was also analyzed.

3.1. The SAC-SMA model

The SAC-SMA model is the most common operational rainfall-runoff model of the National Weather Service River Forecast System (NWSRFS). The SAC-SMA model is a conceptually based lumped rainfall-runoff model which represents spatially heterogeneous runoff processes for river basins at scales ranging from a few hundred to a few thousand square kilometers. There are strong physical arguments to support the model. The model has six soil moisture states and 16 parameters, not counting the 12 monthly adjustment factors of potential evaporation. Most of the parameters have to be calibrated using historical hydrometeorological data.

Partitioning of rainfall into surface runoff and infiltration into the lower zone layers depends on an available storage of tension and free water in the upper zone. It assumes a saturation-excess mechanism for the tension and free water storages, so that the rainfall, P , above a tension water capacity becomes the excess rainfall, P_{excess} . The excess rainfall above a free water capacity becomes surface runoff, R_s ,

$$P_{\text{excess}} = 0, \quad P \leq D_{\text{UZT}} \quad (6)$$

$$P_{\text{excess}} = P - D_{\text{UZT}}, \quad P > D_{\text{UZT}}$$

$$R_s = 0, \quad P_{\text{excess}} \leq D_{\text{UZF}}, \quad (7)$$

$$R_s = P_{\text{excess}} - D_{\text{UZF}}, \quad P_{\text{excess}} > D_{\text{UZF}}$$

where D_{UZT} is a tension water deficit of the upper zone, and D_{UZF} is a free water deficit of the upper zone. All variables of Eqs. (6) and (7) are averaged

over a basin area. After the upper zone storages are filled, rainfall-runoff partitioning is closer to an infiltration-excess type mechanism, and a runoff rate becomes a function of percolation into the lower storages. Interflow is generated depending upon the water contents of the upper and lower zone free water storages. Two components of baseflow are calculated based on supplemental and primary lower zone storages.

3.2. The OSU model

The OSU model was used as the land surface hydrologic parameterization in the Oregon State University one-dimensional planetary boundary layer model (Ek and Mahrt, 1991). The model is based on a finite difference solution of the one-dimensional Richards' equation (Dingman, 1993) in the multi-layer vertical soil column. The Richards' equation is a physically based infiltration model derived from Darcy's law under the assumption of an isotropic, homogeneous soil column. Surface runoff is calculated under the assumption of the Hortonian, infiltration-excess, type of rainfall-runoff partitioning,

$$R_s = \max\{(P - I_{\text{max}}), 0\} \quad (8)$$

A maximum infiltration rate, I_{max} , is estimated based on the water flux at the soil surface:

$$I_{\text{max}} = D(\Theta_s) \frac{\Theta_s - \Theta_1}{\Delta z} + K(\Theta_s) \quad (9)$$

where $D(\Theta_s)$ and $K(\Theta_s)$ are the soil water diffusivity and conductivity under conditions of saturation, Θ_s , Δz is the upper layer thickness, and Θ_1 the water content of the upper soil layer, usually 5–10 cm. Two to ten layer versions of the model were used in the analyses.

The OSU model explicitly accounts for the effect of vegetation on evapotranspiration by the inclusion of a canopy resistance scheme. However, it does not account for the effect of spatial variability in hydrologic variables. Most of the parameters in the OSU model are usually derived using soil and vegetation classification information (Chen et al., 1996). However, a few parameters have to be adjusted if the model is applied to a specific river basin.

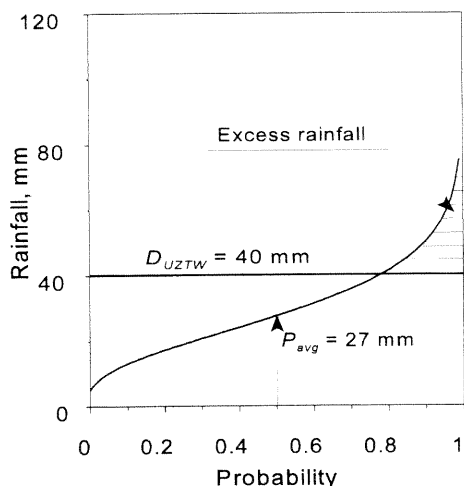


Fig. 2. Probabilistic averaging of excess rainfall using a distribution function of rainfall, where P_{avg} and the distribution function are evaluated at every time step.

3.3. The SWB model

The SWB model has a two-layer structure with both a physical and statistical basis for the model parameters (Schaake et al., 1996). A thin upper layer consists of the vegetation canopy and the soil surface. A lower layer includes both the root zone of the vegetation and the ground water system. Capacities of each layer are model parameters. The supply of water to the lower zone is the excess of precipitation from the upper layer, P_{excess} . This water is available for partitioning into surface runoff and infiltration into the lower layer. The surface runoff equation was derived based on probabilistic averaging of the point infiltration-excess equation (Koren and Kuchment, 1974; Moore, 1985), assuming exponential distribution functions of precipitation and soil moisture capacity,

$$R_s = \frac{P_{excess}^2}{P_{excess} + D_{LZ}(1 - e^{-K_{dt}dt})} \quad (10)$$

where D_{LZ} is the water deficit of the lower zone, dt the simulation time step, and K_{dt} is a model parameter that accounts for the temporal scale. The model has five parameters which are calibrated using historical data.

3.4. Reformulated Sacramento model

The SAC-SMA model was reformulated in order to

account for the spatial variability of rainfall. The reformulated Sacramento model (REF-SAC) replaces actual patterns of rainfall at the river basin scale with a distribution function of rainfall. Mean areal excess rainfall can be estimated assuming that Eq. (6) applies at any point in a basin, the upper zone tension water deficit is uniformly distributed over the basin, and only rainfall is spatially variable,

$$\bar{P}_{excess} = \int_{D_{uztw}}^{\infty} (P - \bar{D}_{uztw})f(P)dP \quad (11)$$

where $f(P)$ is a distribution function of rainfall. Fig. 2 graphically shows the meaning of the reformulation where the SAC-SMA produces zero excess rainfall and therefore zero surface runoff, if the mean areal rainfall of 27 mm is less than the upper zone tension water deficit of 40 mm. However, the reformulated version produces some amount of excess rainfall (shaded area in Fig. 2) depending on the distribution function of rainfall. The same assumptions were used to estimate mean areal surface runoff from Eq. (7) with an additional assumption that point excess rainfall has the same distribution function as rainfall.

To apply the REF-SAC model, a spatial distribution function of rainfall must be estimated at each time step where the SWB model assumes the distribution function to be constant in time. High resolution radar data provides the best available information about the spatial distribution of rainfall which allows the precipitation distribution function to be estimated at every time step. This approach is impossible to apply using only conventional land-based rain gage networks as the spatial structure of the precipitation over headwater basins is not adequately sampled by gage networks. An analysis of the spatial variability of hourly Stage III precipitation grids indicates that a gamma distribution can be used as an approximation to the empirical distribution (Koren, 1993; Schaake et al., 1996),

$$f(P) = \frac{\lambda^\varepsilon}{\Gamma(\varepsilon)} P^{\varepsilon-1} e^{-\lambda P} \quad (12)$$

where λ and ε are the distribution function parameters which can be estimated using mean areal precipitation and coefficient of variation, $C_{v,p}$, and $\Gamma(\varepsilon)$ is the Gamma function. The distribution function parameters were estimated for each time step using only the radar bins with measured rain within the

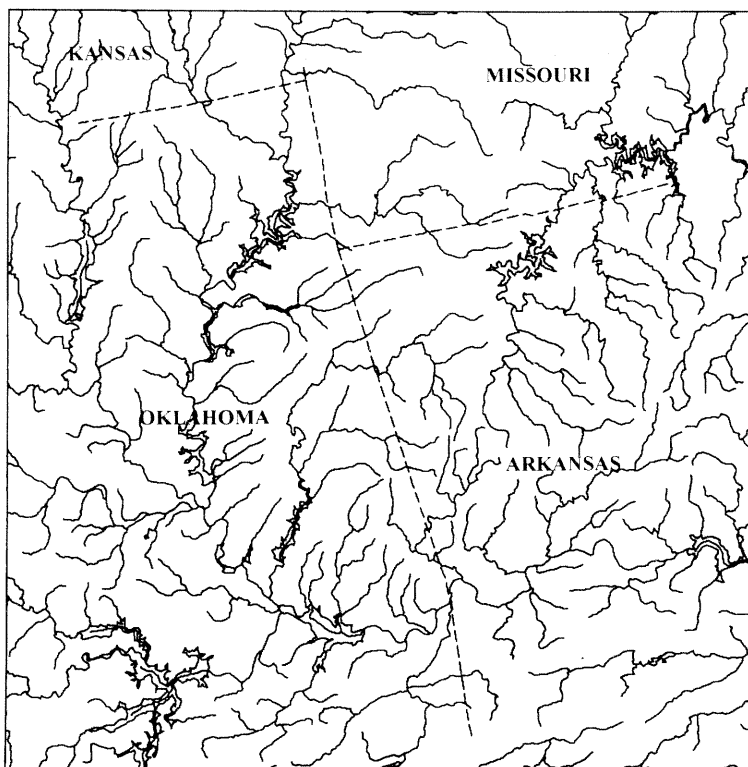


Fig. 3. The test area in the Red river basin over the Oklahoma–Arkansas border, 256×256 km.

simulation area. Simulated excess rainfall and surface runoff were multiplied by the percentage of the rainy area to get average values over an entire basin area.

4. Method and data

Numerical experiments, analogous to the scaling experiments described in Finnerty et al. (1997), were conducted using the four rainfall-runoff models described in the previous section. Hourly rainfall estimates from the high resolution ($4 \text{ km} \times 4 \text{ km}$) Next Generation Weather Radar (NEXRAD) Stage III were used to assess sensitivities of the aggregated model outputs to the grid scale. The selected data set covers the eastern portion of the Tulsa, Oklahoma, river forecasting region and spans a 3-year period from 7 May 1993 to 31 July 1996. This period covers the very wet summer of 1993 which resulted in the “Great Flood of ‘93” in the Midwest.

These gridded precipitation estimates are a multi-sensor product which combines the spatial resolution of the radar data with the ground truth estimates of the gage data. The Stage III technique facilitates the removal of mean field and local biases of the radar derived 1 h precipitation estimates (Shedd and Fulton, 1993; Seo et al., 1998; Seo, 1998). Although radar-based precipitation estimates still have uncertainties, they are far superior compared with rain gage networks in their ability to spatially represent heavy rainfall (Smith et al., 1996). For this study, the determination of proper spatial statistical properties of the rainfall grids is more critical than the accuracy of precipitation estimates.

The test area in the Red river basin over the Oklahoma–Arkansas border, Fig. 3, was gridded into 64×64 rectilinear cells of approximately $4 \text{ km} \times 4 \text{ km}$ in size, which match those of the radar rainfall data. The models were run in a continuous mode for the entire period at grid scales of 4×4 , 8×8 , 16×16 , 32×32 ,

Table 2
Sub-basin scales in the 64×64 NEXRAD bin test area

Sub-basin scale, km	Sub-basin size, km ²	Number of sub-basins in the test area
4 × 4	16	4096
8 × 8	64	1024
16 × 16	256	256
32 × 32	1024	64
64 × 64	4096	16
128 × 128	16 384	4
256 × 256	65 536	1

64×64 , 128×128 , and 256×256 km² by using average rainfall over each synthetic sub-basin defined by the grid scale. Each component of the model output was then averaged over aggregation scales of 8×8 , 16×16 , 32×32 , 64×64 , 128×128 , and 256×256 km². Table 2 shows the number of sub-basins which were used in aggregation of model outputs at a different sub-basin scale.

The SAC-SMA model parameters were calibrated using historical data for the 795 km² headwater basin of the Baron Fork of the Illinois river at Eldon,

Oklahoma (Finnerty et al., 1997). The calibrated basin is close to the 32×32 km synthetic sub-basin scale and those parameters were distributed uniformly over the entire test area. A priori parameter estimates were used to run the OSU and SWB models. Only a few parameters of those models were manually adjusted to get unbiased total runoff for the entire period, and to generate a surface–subsurface runoff ratio close to values simulated by the SAC-SMA model.

5. Results and discussion

5.1. Comparison of different model results

Runoff components generated by each model (a 10-layer version of the OSU model was used in this test) were cumulated for the entire period and averaged over the test area, 256×256 km. Fig. 4 is a plot of the relative change in the surface runoff volume simulated by the different models over the 3-year period as a function of the grid scale. Surface runoff changes at each grid scale are defined as the difference between the total cumulated surface runoff at that scale and the

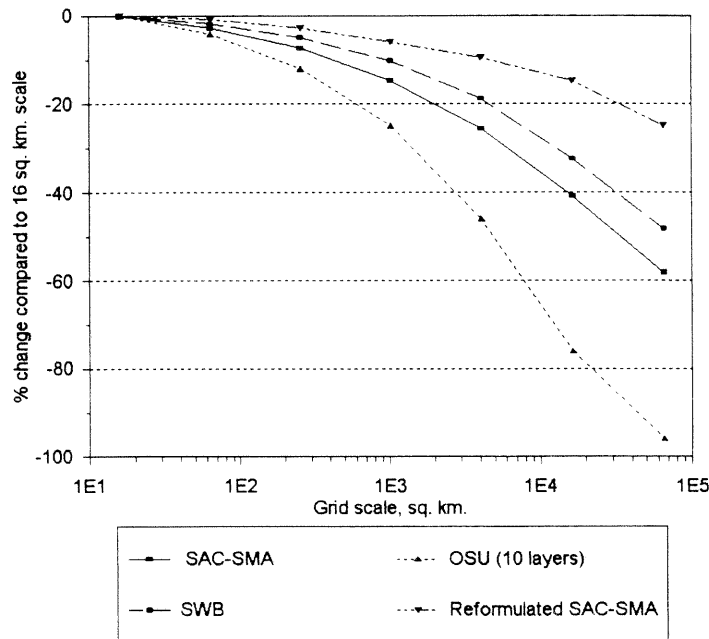


Fig. 4. Scale dependency of surface runoff, simulated by different models and expressed in percent change in surface runoff as compared with the finest scale value. Statistics are aggregated for all synthetic sub-basins in the test area continuously over the 3.5-year period.

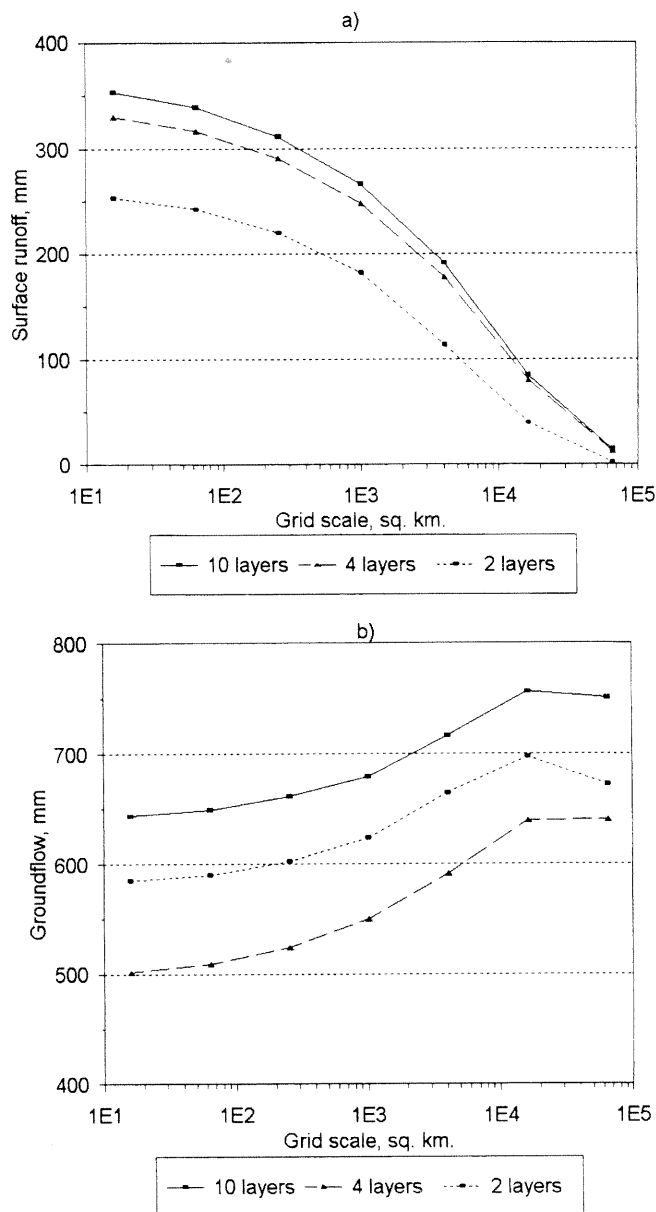


Fig. 6. Scale dependency of the OSU model outputs generated using different number of soil layers: (a) Surface runoff; (b) Groundflow; (c) Evapotranspiration; and (d) Soil moisture change.

As expected, the SWB model was less scale dependent than the SAC-SMA and OSU models as its infiltration equation implicitly accounts for the spatial variability of rainfall. However, reduction of surface runoff at the larger scales exceeded 30%. One of the

reasons for this reduction at the larger scales was that the areas covered by rain were significantly reduced at the 128×128 and 256×256 km scales, 64% and 45%, respectively. Whereas, Table 1 shows, the finer 4×4 and 8×8 km² scales have 100% and

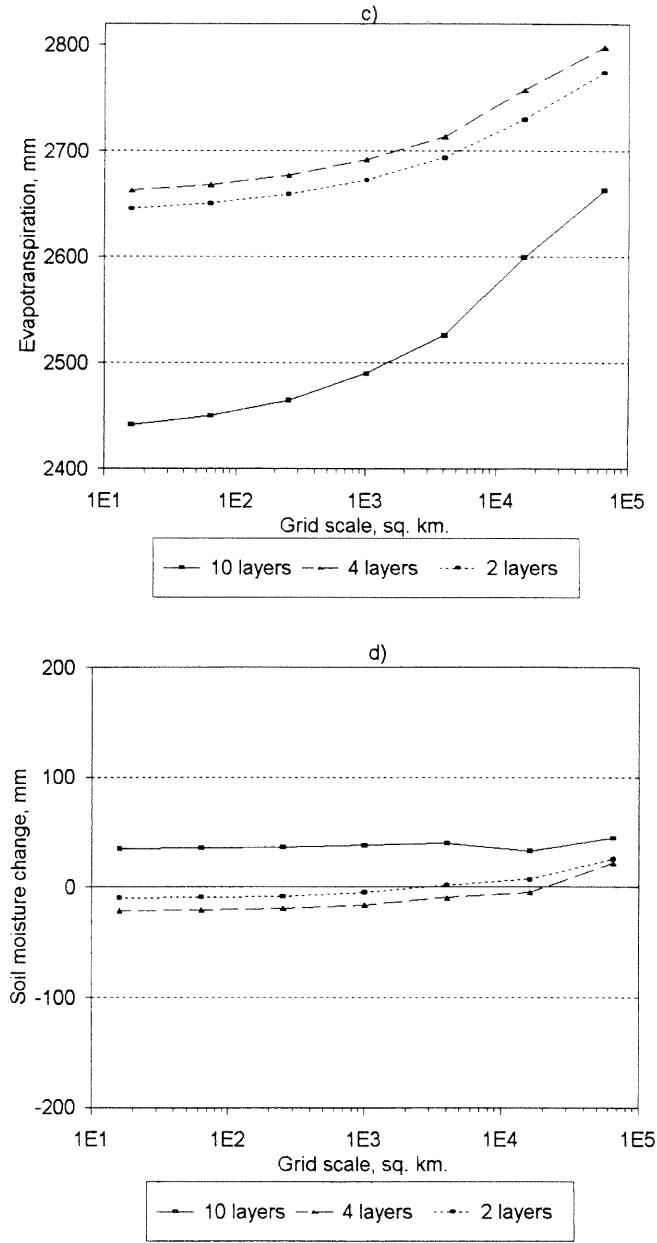


Fig. 6. (continued)

98% covered areas, respectively. The SWB model assumes that rain covers the entire area and this assumption is clearly violated at the larger spatial scales.

The reformulated SAC-SMA model was found to

be the least sensitive to grid scale. At the largest scale of 256×256 km the model underestimated surface runoff by about 20% compared with 60% by the original SAC-SMA model. As the spatial distribution of rainfall and rain coverage were estimated at each time

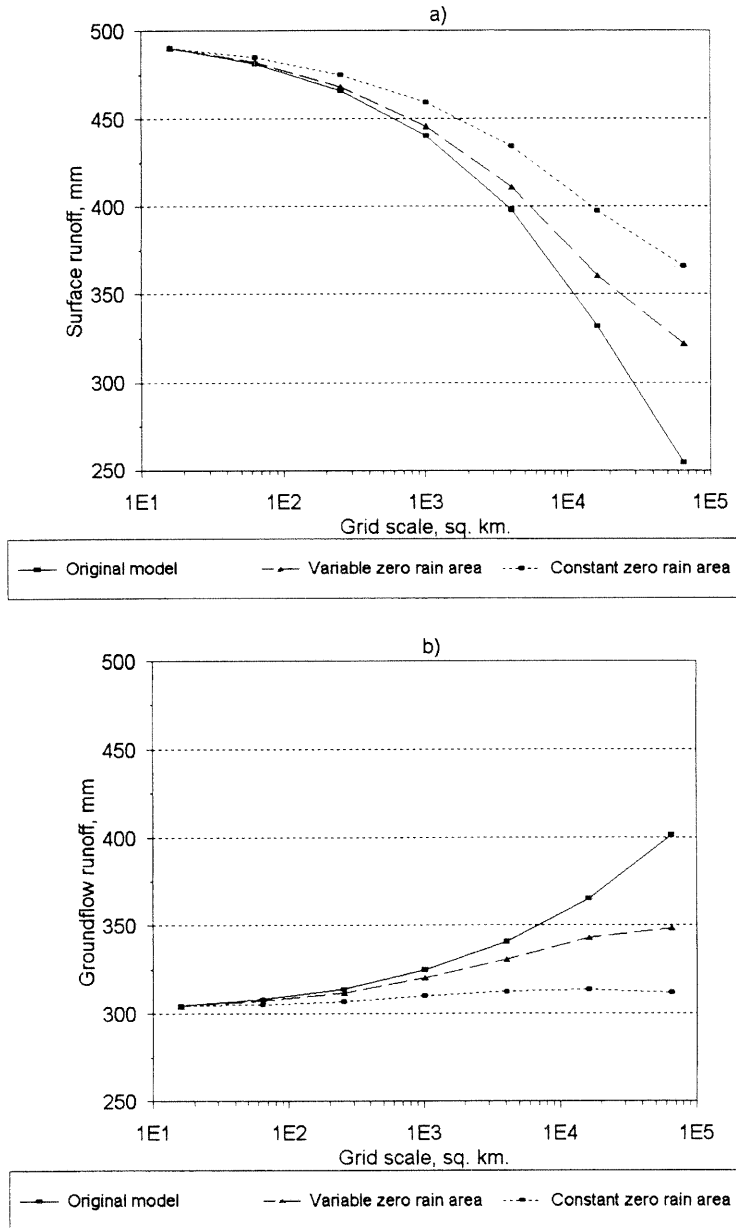


Fig. 7. Scale dependency of the SWB model outputs generated using different representation of fractional rain coverage: (a) Surface runoff; (b) Groundflow; (c) Evapotranspiration; and (d) Soil moisture change.

step, the reformulated SAC-SMA model produced more reasonable results over a wide range of spatial scales.

As seen in Fig. 5, all models showed much less scale dependency in total runoff. Total runoff was

calculated as a sum of surface and groundwater flows for the OSU and SWB models, and as a sum of six runoff components: surface, interflow, primary and supplemental baseflow, permanent and variable impermeable area flow, for the SAC-SMA model.

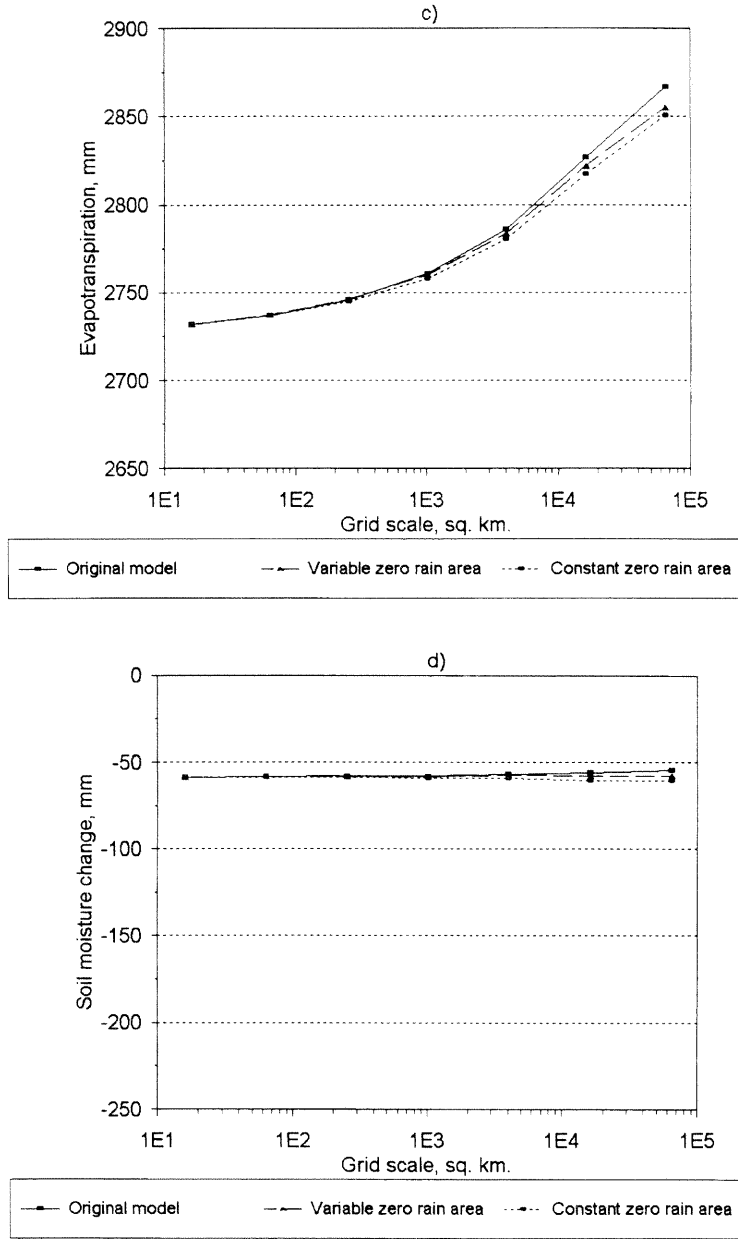


Fig. 7. (continued)

The total runoff reduction was about three times less than the surface runoff reduction. The models ranking based on the scale dependency of total runoff were close to that based on the surface runoff dependency order: the OSU model was the most scale dependent,

and the reformulated SAC-SMA model was the least scale dependent. The only difference was that the SAC-SMA model became a little less scale dependent than the SWB model. There is less scale dependency in the total runoff as surface and subsurface

components usually change in opposite directions as the scale increases. That is, the surface runoff decreases at the larger scales while the subsurface component increases. The SAC-SMA model multi-interaction between runoff components reduces the effect of the surface runoff scale dependency in the total runoff significantly.

5.2. The OSU model results using different number of soil layers

The partitioning of rainfall into runoff and losses, and redistribution of soil moisture by the OSU model depends on the calculation of soil moisture fluxes. Different numbers of soil layers can lead to different estimates of the soil moisture fluxes and, as a result, to different scale sensitivities of the model. In practical applications only a few soil layers are often used (Chen et al., 1996).

Three versions of the OSU model were analyzed in this scale study: 10-, four-, and two-layer versions. The same thicknesses of the top layers were used in all versions, as shown in Table 3. The finer resolutions of the top layers were selected to get better estimates of soil moisture fluxes (Mahrt and Pan, 1984).

The water balance components, accumulated for the total period and aggregated over the test area, are plotted against grid scale in Figs. 6a–d. Generally, surface and groundwater runoff volumes decreased, and evapotranspiration increased when decreasing the number of soil layers. However, groundwater runoff of the two-layer version was higher than that of the four-layer version, Fig. 6b. Feedback mechanisms of the model compensate for the reduction in surface runoff by significantly increasing the groundwater runoff. Evapotranspiration in the two-layer version was a little lower than the evapotranspiration in the four-layer version, as seen in Fig. 6c. The soil moisture change for the total period differs greatly in different versions, as shown in Fig. 6d. The 10-layer version shows small changes in soil moisture at different scales. Overall, increasing the number of layers leads to a little more scale dependency in runoff and evapotranspiration, although long-term soil moisture change tends to be more stable in the most multi-layer version.

5.3. Fraction of rainy area in the SWB model

As stated previously, the SWB model results at larger scales depended on the fraction of the rainy area. Surface runoff in Eq. (11) of the SWB model can be generalized to account for zero rain areas. If rainy area patterns do not correlate in time, soil moisture states over the entire area can be used to estimate surface runoff from rainy areas. Then Eq. (11) of the SWB model can be generalized to account for a fraction of rainy area, λ ,

$$R_s = \frac{P_{excess}^2}{P_{excess} + \lambda D_{LZ}(1 - e^{-K_d dt})}. \quad (13)$$

The fraction of rainy area was calculated for each hourly precipitation grid at the selected grid scales. The fraction in this case varies with time and grid scale. Time constant values of the rainy area fraction values from Table 1, which are weighted averages for the 3-year period, were also used in the analyses. Figs. 7a–d display water balance components simulated by the SWB model using different versions of rainy area representation:

1. total coverage of an area (original model);
2. constant fractions of the rainy area from Table 1; and
3. a variable fraction calculated at each time step using radar data.

Both surface and groundwater runoffs were sensitive to the fraction of rainy area. At the largest scale, differences in runoffs with different versions of the model were as much as 30%–40%, as shown in Fig. 7a and b. However, evapotranspiration and soil moisture changes differ little as a function of rainy area representation from scale to scale, as shown in Fig. 7c and d. Increased surface runoff with decreased rainy areas was compensated by decreased groundwater runoff. Differences in soil moisture change for the total period from different versions were less than 2%.

The two SWB versions that account for the rainy area fraction are less scale dependent as compared to the original model. However, it was surprising that the version with a time constant rainy area was less sensitive to the grid scale compared to the time variable coverage version. A possible reason for this is that the SWB

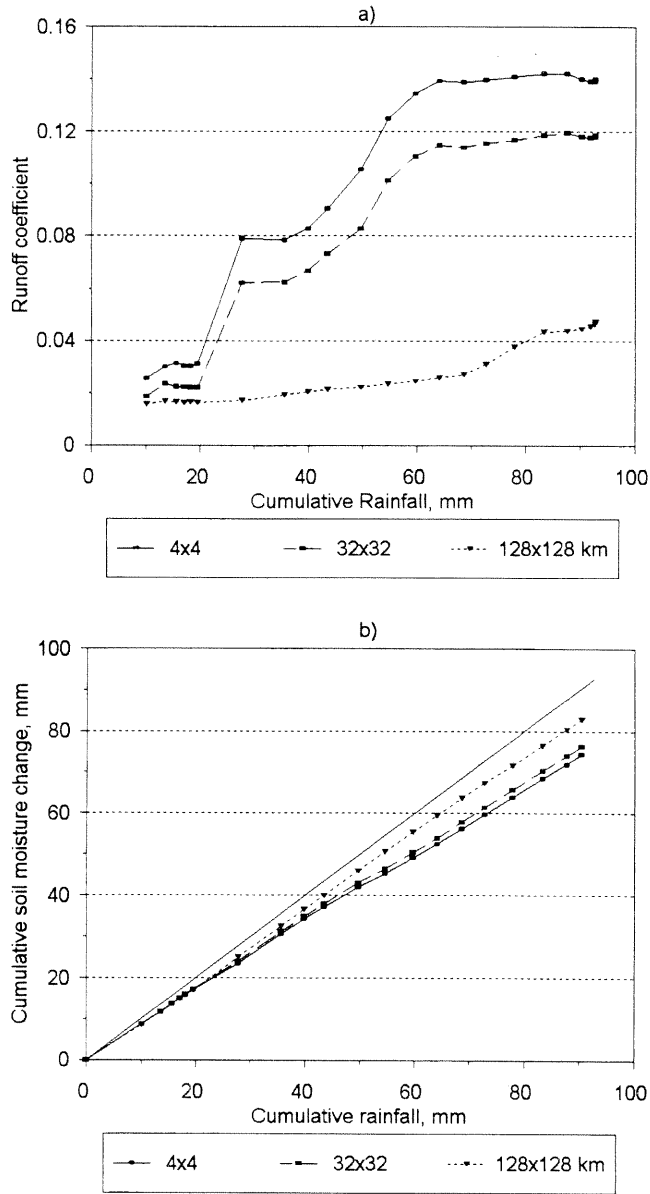


Fig. 8. Dynamics of the SAC-SMA model outputs during a single flood event (04/12/94) generated at different scales: (a) Runoff coefficient versus cumulative rainfall and (b) Soil moisture change versus cumulative rainfall.

model accounts for rainy areas without regard to their location. Rainy area location becomes critical with decreasing a coverage fraction. Probabilistic spatial averaging cannot account for the mapping

of current precipitation distribution onto prior soil moisture distribution. It is more important for the variable version when a coverage fraction varies significantly in time.

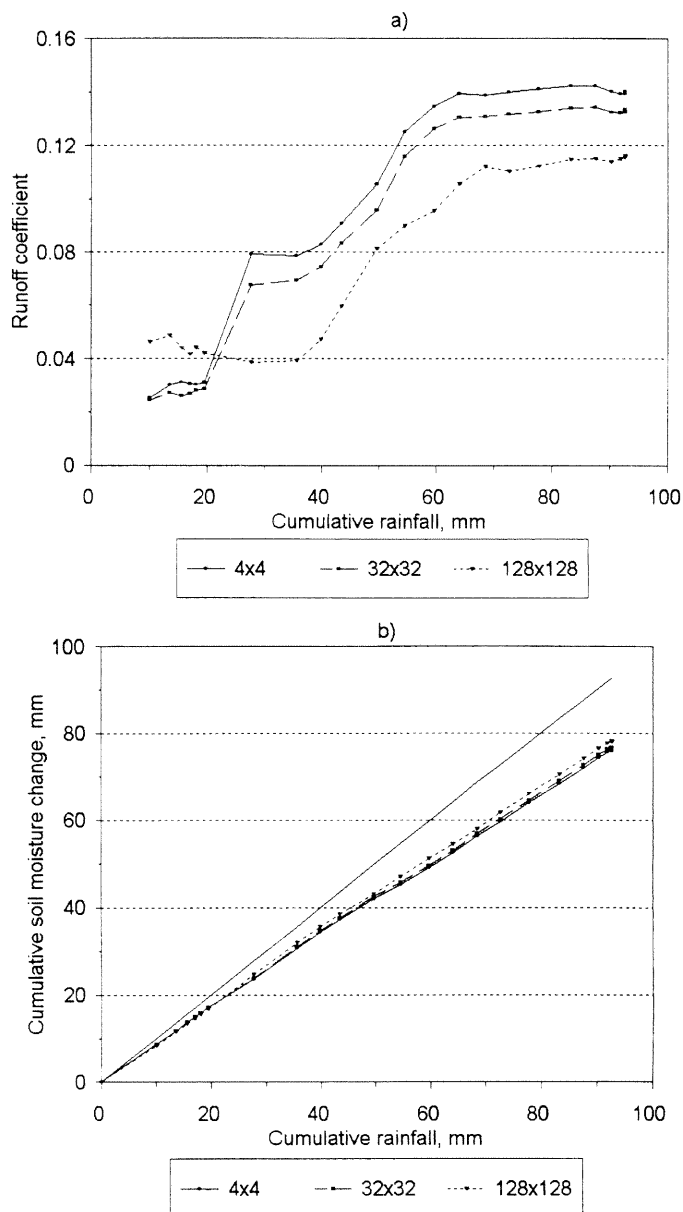


Fig. 9. Dynamics of the reformulated SAC-SMA model outputs during a single flood event (04/12/94) generated at different scales: (a) Runoff coefficient versus cumulative rainfall and (b) Soil moisture change versus cumulative rainfall.

5.4. Rainfall-runoff partitioning in the SAC-SMA model

The importance of the rainfall-runoff partitioning mechanism is seen during flood events. Fig. 8a is a

plot of the runoff coefficient during a specific flood event, 12 April 1994, simulated using total channel inflow from the SAC-SMA model outputs at different grid scales. The runoff coefficient is defined as the ratio of accumulated runoff to accumulated

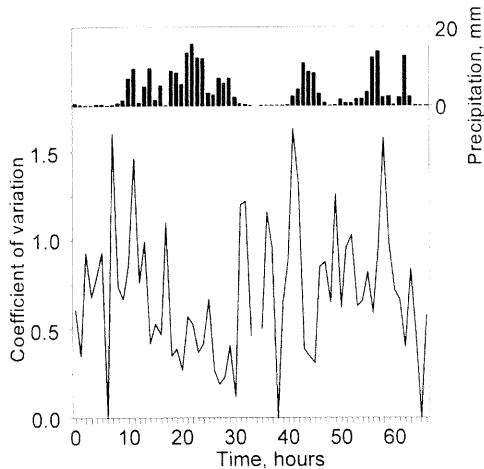


Fig. 10. Temporal variability of the coefficient of spatial variation of hourly precipitation in the test area.

precipitation, for a given time interval. At the beginning of the flood, when initial losses are satisfied, the runoff coefficient is rather stable and does not vary much from scale to scale. Once initial losses have been satisfied, the runoff coefficient varies significantly over different scales with the highest values at the finest scale. Most of the rainfall during the storm was stored in the soil at the 128×128 km scale, and the runoff coefficient was close to zero during the entire flood event. As a result, soil moisture content increased during the flood and was the greatest for the lowest resolution as shown in Fig. 8b.

The reformulated SAC-SMA model showed less scale dependency in rainfall-runoff partitioning. The range of the runoff coefficient variability across scales was narrower during the same flood event, as shown in Fig. 9a. The 128×128 km scale has a higher runoff coefficient at the beginning of the flood event because of different soil moisture states from the continuous run. Soil moisture content at the end of the flood was close for all grid scales, as shown in Fig. 9b.

The importance of the temporal variability in the distribution function of precipitation can be seen by comparing simulation results from the reformulated SAC-SMA and SWB models. Although the SWB model accounts for the spatial variability of rainfall, it assumes that there is no temporal variability in the distribution function of precipitation. The actual distribution of precipitation varies from one storm to

another and during a single storm. Fig. 10 is an example of temporal variability of the coefficient of spatial variation of hourly precipitation during a few storm events in the test area. This temporal variability of heterogeneity of precipitation is accounted in the reformulated SAC-SMA model that leads to the reduction in its scale dependency.

6. Conclusions

Four different lumped hydrological models with varied complexity of infiltration parameterizations were used in the analyses of the scale dependency of model outputs to the spatial variability of rainfall. Two models, the SAC-SMA and OSU, are point type models that do not account for the spatial variability of rainfall within the basin. Two other models, the SWB and reformulated SAC-SMA, account for the precipitation spatial variability by using probabilistic averaging of point processes. The high-resolution, 4×4 km, hourly rainfall estimates for the 3.5-year period from the NEXRAD radar were used in the study. All land-surface characteristics and model parameters were assumed to be constant over the entire test area to exclude their possible contribution to results of the rainfall variability study.

Model generated runoff, soil moisture, and evapotranspiration were compared at different grid scales when averaged over the entire test area, 256×256 km. All models produced less surface and total runoff, and more evapotranspiration with increasing scale size. Rainfall variability was a primary factor of runoff reduction at the smaller scales, and rainfall coverage became a major factor at the larger scales.

Although all selected models were scale dependent, the level of dependency varied significantly with different formulations of the rainfall-runoff partitioning mechanism. The point type OSU model with a pure infiltration-excess mechanism was the most sensitive to the rainfall spatial variability. The better representation of the soil moisture profile by using more soil layers did not reduce scale dependency. Mixed saturation/infiltration-excess type models, such as the original and reformulated SAC-SMA models, were less sensitive to the scale. The rainfall rate induced scale dependency of the fast runoff components on the rainfall rate was reduced

significantly during the first phase of the flood when a saturation-excess mechanism was dominated.

Probabilistic averaging of the point processes reduces scale dependency, as demonstrated by the SWB and reformulated SAC-SMA models. Effectiveness of the probabilistic averaging varies depending on the scale, and was reduced with increased scale size as rainfall coverage and rain area locations became an important factor. Continuous assimilation of a distribution function of rainfall, and a rainy area fraction significantly reduced scale dependency of the SAC-SMA model at the larger scales.

All models showed less scale dependency in total runoff compared with surface runoff as surface and subsurface runoff components usually changed in opposite directions as the scale increased. That is, the surface runoff decreased at the larger scales while the subsurface component increased. It suggests that neglecting the subsurface-groundwater component by compensating for it in a surface runoff component can lead to an increase in the model scale dependency.

The analysis was focused on the scale dependency of different models rather than on their performances compared to measured data. If well calibrated, the more scale-dependent model may give better results at the applied basin scale than the less scale-dependent model. The importance of the scale sensitivity of the model depends on the specific application. In the local rainfall-runoff forecasting over dense gauge regions it is important to use a model that showed high accuracy in rainfall-runoff simulations, and could be calibrated properly using historical data. Less scale-dependent models are desirable when rainfall-runoff simulations are performed over large ungaged regions and there is a need in transferring of model parameters from different size basins.

References

- Avissar, R., 1995. Scaling of land-atmosphere interactions: an atmospheric modeling perspective. *Hydrological Processes*, 10th Anniversary Issue: 3–19.
- Beven, K.J., Wood, E.F., 1993. Flow routing and the hydrological response of channel networks. In: Beven, K.J., Kirkby, M.J. (Eds.), *Channel Network Hydrology*, John Wiley, Chichester, pp. 99.
- Burnash, R.J.C., 1995. The NWS river forecast system – catchment modeling. In: Singh, V.P. (Ed.), *Computer Models of Watershed Hydrology*, Water Resources Publ, Highlands, Colorado, pp. 311.
- Chen, F., Mitchell, K., Schaake, J., Xue, Y., Pan, H.-L., Koren, V., Duan, Q.Y., Ek, M., Betts, A., 1996. Modeling of land surface evaporation by four schemes and comparison with FIFE observations. *J. Geophys. Res.* 101 (D3), 7251–7268.
- Dingman, S.L., 1993. *Physical Hydrology*. Prentice Hall, Englewood Cliffs, NJ.
- Ek, M., Mahrt, L., 1991. OSU 1-D PBL model User's Guide. Department of Atmospheric Sciences, Oregon State University, Corvallis, Oregon.
- Entekhabi, D., Eagleson, P.S., 1989. Land surface hydrology parameterization for atmospheric general circulation models including subgrid scale spatial variability. *J. Clim.* 2, 816–831.
- Finnerty, B.D., Smith, M.B., Seo, D.-J., Koren, V.I., Moglen, G., 1997. Sensitivity of the Sacramento soil moisture accounting model to space-time scale precipitation inputs from NEXRAD. *J. Hydrol.* 203 (1–4), 21–38.
- IAHS/UNESCO, 1970. *Proceedings of the Symposium on the Results of Research on Representative and Experimental Basins*, Publication No 96, Vol. 1. Wellington, UK.
- Klemes, V., 1983. Conceptualization and scale in hydrology. *J. Hydrol.* 65, 1–23.
- Koren, V.I., 1993. The potential for improving lumped parameter models using remotely sensed data. *Proceedings of the 13th Conference on Weather Analysis and Forecasting*, Vienna, Virginia, 2–6 August, 1993, AMS/WMO/NWA, pp. 397–400.
- Koren, V.I., Kuchment, L.S., 1974. Physicostatistical model of rainfall flood formation and determination of its parameters. *Proceedings of the Warsaw Symposium on Mathematical Models in Hydrology*, IAHS/UNESCO, Publication No 101, Vol. 2, Warsaw, July 1971, Poland.
- Kouwen, N., Garland, G., 1989. Resolution consideration in using radar data for flood forecasting. *Can. J. Civil Engng* 16, 279–289.
- Loague, K.M., 1988. Impact of rainfall and soil hydraulic property information on runoff predictions at the hillslope scale. *Water Resour. Res.* 24 (9), 1501–1510.
- Mahrt, L., Pan, H., 1984. A two-layer model of soil hydrology. *Boundary Layer Meteorol.* 29, 1–20.
- Mein, R.G., Brown, B.M., 1978. Sensitivity of parameters in watershed models. *Water Resour. Res.* 14 (2), 299–303.
- Moore, R.J., 1985. The probability-distributed principle and runoff production at point and basin scales. *Hydrol. Sci. J.* 30 (2), 273–297.
- Obled, Ch., Wendling, J., Beven, K., 1974. The sensitivity of hydrological models to spatial rainfall patterns: an evaluation using observed data. *J. Hydrol.* 159, 305–333.
- Ogden, F.L., Julien, P.Y., 1994. Runoff model sensitivity to radar rainfall resolution. *J. Hydrol.* 158, 1–18.
- Schaake, J.C., Koren, V.I., Duan, Q.Y., Mitchell, K., Chen, F., 1996. Simple water balance model for estimating runoff at different spatial and temporal scales. *J. Geophys. Res.* 101 (D3), 7461–7475.
- Seo, D.-J., Fulton, R.A., Breidenbach, J.P., 1998. Rainfall

- estimation in the WSR-88D era for operational hydrologic forecasting in the National Weather Service, Preprints, Special Symposium on Hydrology, American Meteorological Society, Boston, MA.
- Seo, D.-J., 1998. Real-time estimation of rainfall fields using radar rainfall and rain gage data. *J. Hydrol.* 208, 37–52.
- Shah, S.M.S., O'Connell, P.E., Hosking, J.R.M., 1996. Modeling the effects of spatial variability in rainfall on catchment response. 2: experiments with distributed and lumped models. *J. Hydrol.* 175, 89–111.
- Shedd, R.C., Fulton, R.A., 1993. WSR-88D precipitation processing and its use in National Weather Service hydrologic forecasting. Proceedings of ASCE International Symposium on Engineering Hydrology, San Francisco, CA, 25–30 July 1993.
- Smith, J.A., Seo, D.-J., Baeck, M.L., Hudlow, M.D., 1996. An intercomparison study of NEXRAD precipitation estimates. *Water Resour. Res.* 32 (7), 2035–2045.
- WMO, 1975. Intercomparison of conceptual models used for hydrological forecasting, Operational Hydrology Report, No 7, WMO-429, Geneva.
- Wood, E.F., Sivapalan, M., Beven, K.J., 1990. Similarity and scale in catchment storm response. *Rev. Geophys.* 28(1), 1–18.
- World Climate Research Program (WCRP), 1992. Implementation plan for GEWEX Continental-Scale International Project (GCIP), WCRP-67, WMO/TD-461, Geneva.

Notes to contributors

A detailed *Guide for Authors* is available upon request from the Publisher, Elsevier Science Ireland Ltd., Elsevier House, Brookvale Plaza, East Park, Shannon, Co. Clare, Ireland. Tel.: (353) 61 709652, Fax: (353) 61 709110, e-mail: a.glynn@elsevier.ie, and will also be printed each year (for 1999: Vol. 214, Nos. 1–4). Please pay attention to the following notes:

Language

The official language of the journal is English.

Preparation of the text

- (a) The manuscript should preferably be prepared on a word processor and printed with double spacing and wide margins and include an abstract of not more than 500 words.
- (b) The title page should include the name(s) of the author(s), their affiliations, fax and e-mail numbers. In case of more than one author, please indicate to whom the correspondence should be addressed.

Keywords

Authors should provide 4 to 6 keywords. These must be taken from the most recent American Geological Institute GeoRef Thesaurus and should be placed beneath the abstract.

References

- (a) References in the text consist of the surname of the author(s), followed by the year of publication in parentheses. All references cited in the text should be given in the reference list and vice versa.
- (b) The reference list should be in alphabetical order and on sheets separate from the text.

Tables

Tables should be compiled on separate sheets and should be numbered according to their sequence in the text.

Illustrations

- (a) All illustrations should be numbered consecutively and referred to in the text.
- (b) Drawings should be lettered throughout, the size of the lettering being appropriate to that of the drawings, but taking into account the possible need for reduction in size. The page format of the journal should be considered in designing the drawings.
- (c) Photographs must be of good quality, printed on glossy paper.
- (d) Figure captions should be supplied on a separate sheet.
- (e) If contributors wish to have their original figures returned this should be requested at proof stage at the latest.
- (f) Colour figures can be accepted providing the reproduction costs are met by the author. Please consult the publisher for further information.

Proofs

One set of proofs will be sent to the corresponding author, to be checked for typesetting/editing. The author is not expected to make changes or corrections that constitute departures from the article in its accepted form.

Page charges and reprints

There will be *no page charge*. Each author receives with his galley proofs a reprint order form which must be completed and returned to the Publisher with the proofs, Elsevier Science Ireland Ltd., Elsevier House, Brookvale Plaza, East Park, Shannon, Co. Clare, Ireland, Tel.: (353) 61-709652, Fax: (353) 61-709110, e-mail: a.glynn@elsevier.ie. Additional reprints (minimum 100) can be ordered at quoted prices. *Fifty reprints* of each article are supplied *free of charge*.

Submission of manuscripts

Authors are requested to submit, with their manuscripts, the names and addresses of *four* potential referees. One original and two copies should be submitted to: Editorial Office, Journal of Hydrology, P.O. Box 1930, 1000 BX Amsterdam, The Netherlands. The indication of a fax and e-mail number on submission of the manuscript could assist in speeding communications. Illustrations: Please note that on submission of a manuscript **three** sets of all photographic material printed **sharply on glossy paper** or as **high-definition laser prints** must be provided to enable meaningful review. Photocopies and other low-quality prints will not be accepted for a review. Submission of an article is understood to imply that the article is original and unpublished and is not being considered for publication elsewhere. Upon acceptance of an article by the journal, the author(s) will be asked to transfer the copyright of the article to the publisher. This transfer will ensure the widest possible dissemination of information.

Authors in Japan please note: Upon request, Elsevier Science K.K. will provide authors with a list of people who can check and improve the English of their paper (*before* submission). Please contact our Tokyo office: Elsevier Science K.K., 9–15 Higashi-Azabu 1-chome, Minato-ku, Tokyo 106-0044. Tel: (03)-5561-5033, Fax (03)-5561-5047.

Submission of electronic text

In order to publish the paper as quickly as possible after acceptance, authors are encouraged to submit the final text also on a 3.5" or 5.25" diskette. Both double density (DD) and high density (HD) diskettes are acceptable. Make sure, however, that the diskettes are formatted according to their capacity (HD or DD) before copying the files onto them. Similar to the requirements for manuscript submission, main text, list of references, tables and figure legends should be stored in separate text files with clearly identifiable file names. The format of these files depends on the word processor used. Texts made with DisplayWrite, MultiMate, Microsoft Word, Samna Word, Sprint, Volkswriter, Wang PC, WordMARC, WordPerfect, Wordstar, or supplied in DCA/RFT, or DEC/DX format can be readily processed. In all other cases the preferred format is DOS text or ASCII. It is essential that the name and version of the wordprocessing program, type of computer on which the text was prepared, and format of the text files are clearly indicated. Authors are requested to ensure that the contents of the diskette correspond exactly to the contents of the hard copy manuscript. Discrepancies can lead to proofs of the wrong version being made. The word processed text should be in single column format. Keep the layout of the text as simple as possible; in particular, do not use the word processor's options to justify or to hyphenate the words. If available, electronic files of the figures should be included on a separate floppy disk.

